2.1.3. In Situ Methane Measurements

During 1993, in situ measurements of atmospheric CH_4 continued with a frequency of 60 samples per day at MLO and BRW. The precision of the measurements (~0.2%) is limited in part by variations in laboratory temperature that affect the flow rate of the flame ionization detector (FID) fuel, H_2. In Figure 2.7, reference peak heights are plotted for a 2-wk period at MLO. A distinct diurnal cycle is evident. This is observed because the H_2 cylinder is stored in an attached, but unheated portion of the MLO laboratory, where temperature mearly tracks the outside temperature. The low pressure setting of the cylinder regulator determines the H_2 flow rate at the FID, and is sensitive to temperature. Fortunately, the temperature change is slow enough that the measurements are not affected too severely. At BRW, variations in reference peak height are even larger than at MLO, but these probably cannot be fully explained by variations in laboratory temperature. A temperature controlled, heated module is being built where high-precision pressure regulators will be housed, and these will determine the gas flow rates without the effects of varying room temperature. The gas sample valve will be moved from the GC oven into the heated module. The benefit of this is that the GC oven can then be used to bake out the silica gel and molecular sieve columns at much higher temperatures than currently achievable with the valve inside the oven since the valve can be damaged by heating above 150°C. A GC containing these modifications should be installed at MLO during 1994.

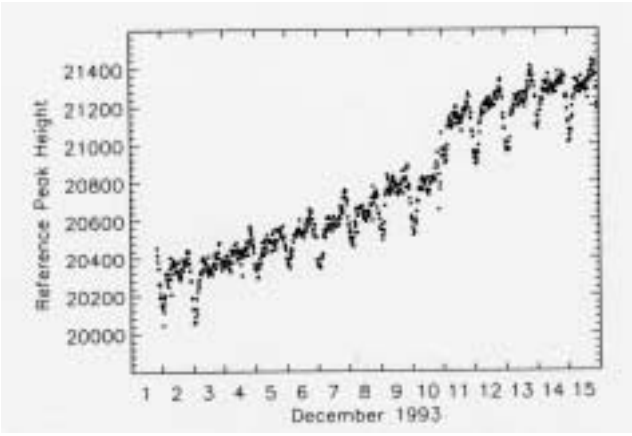

Fig. 2.7. Methane reference gas peak heights, in counts (where 1 count = 0.125 mV), for a 2-wk period at MLO. Peak heights were quantified with an HP3393A integrator.

Edited, unconstrained, daily mean CH_4 mixing ratios are shown in Figure 2.8*a* for BRW and 2.8*b* for MLO. Features in the data in 1993 are similar to previous years. At MLO, CH_4 is highly variable on time scales of days to weeks because of variations in atmospheric transport [*Harris et al.*, 1992]. At BRW, most of the highest values are because of local CH_4 emissions. At both observatories, CH_4 is lower during summer than during winter because of chemical destruction by hydroxyl radical. Methane seasonal cycles at MLO and BRW are explored in more detail below.

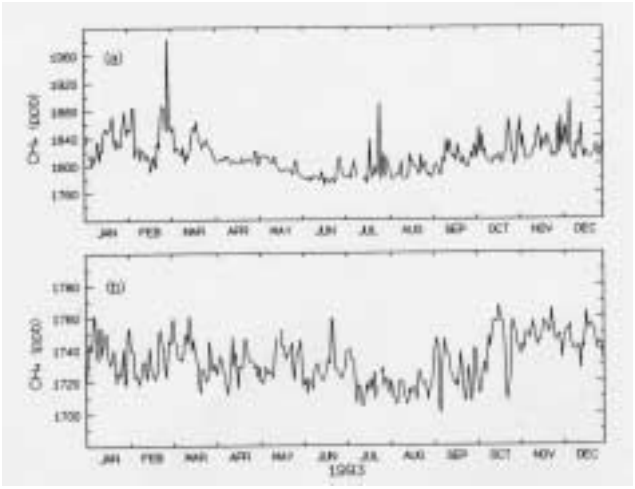

Fig. 2.8. Daily mean CH_4 mixing ratios in ppb for (a) BRW and (b) MLO for 1993. The data are unconstrained, but have undergone a quality control step to ensure that the analytical instrument was working optimally when they were obtained [*Masarie et al.*, 1991].

In Figure 2.9*a*, standard deviations from the daily means are shown for MLO. The maximum frequency occurs at s ~4.5 ppb, and the distribution has a relatively long tail. The shape of the distribution depends on the instrument precision and natural variations in the CH_4 mixing ratio at the sampling site. At MLO a diurnal cycle in the methane mixing ratio sometimes exists with a peak-to-peak amplitude of ~10 ppb because of the upslope and downslope wind regimes [*Peterson and Rosson*, 1993]. Daily means were also calculated for times of predominantly downslope conditions (0000-0700 LST) that represent free tropospheric air. The associated standard deviations are shown in Figure 2.9*b*. Note that the maximum in the distribution shifts to s ~2.5 ppb, close to the instrument precision, and much of the long tail is no longer present. Still, the distribution is not Gaussian. This results because natural variations in CH_4 mixing ratios, due to variations in transport, are still present.

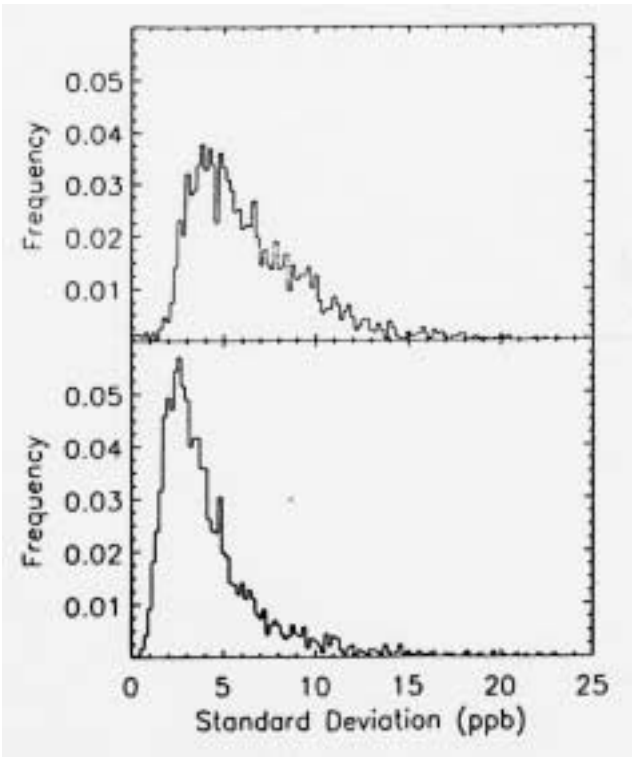

Fig. 2.9. (*a*) Histogram of standard deviations for MLO daily means calculated from hourly averages. (*b*) Same as a, but data were constrained to time periods between 0000 to 0700 LST to capture downslope conditions. In both cases, there is one datum lying outside the range plotted.

The CH_4 time-series is a combination of three primary factors: (1) a long-term trend because of the small imbalance between CH_4 sources and sinks; (2) an annual cycle because of the seasonality of some CH_4 sources and the CH_4 photochemical sink; and (3) short-term variations occurring on time scales of days to weeks due to variations in atmospheric transport at the sampling sites. These components were separated for analysis by first fitting a quadratic polynomial to the data to represent the long-term trend and a series of four harmonics to represent the average seasonal cycle.

$$f(t) = a_1 + a_2 t + a_3 t^2 + \sum_{i=1}^{4} [a_{2i+2} \sin(2\pi i t) + a_{2i+3} \cos(2\pi i t)] \quad (1)$$

Digital filtering of the residuals is applied to determine short-term variations (filter cut off = 4.56 cycles yr^{-1}) and interannual variations in the long-term trend (filter cut off = 0.55 cycles yr^{-1}).

The average, detrended seasonal cycles for BRW (*a*) and MLO (*b*) are shown as the solid curves in Figure 2.10. These curves show only the fundamental and harmonic frequencies. The filled circles are detrended monthly means (±1s) determined from a smooth curve fitted to daily means. At MLO, the average position of the seasonal maximum was at the end of November, and the seasonal minimum was during the first week of August. The average peak-to-peak seasonal cycle amplitude was 25.1 ppb. At BRW, the average position of the seasonal maximum was at the beginning of February, and the minimum occurred on average at the end of June. The average seasonal-cycle amplitude at BRW was 47.2 ppb. Minimum values at both sites occurred during the summer when the photochemical sink was most active. The minimum at BRW preceded MLO by about 6 weeks. This is probably due to the seasonality of CH_4 emissions from boreal wetlands that become active during early summer and reach their peak emissions during late summer, somewhat canceling the effect of chemical destruction. Although the emissions from boreal wetlands and rice agriculture also play a part in determining the phase and amplitude of the CH_4 seasonal cycle at MLO, the effect is smaller due to the large distances between MLO and the source regions.

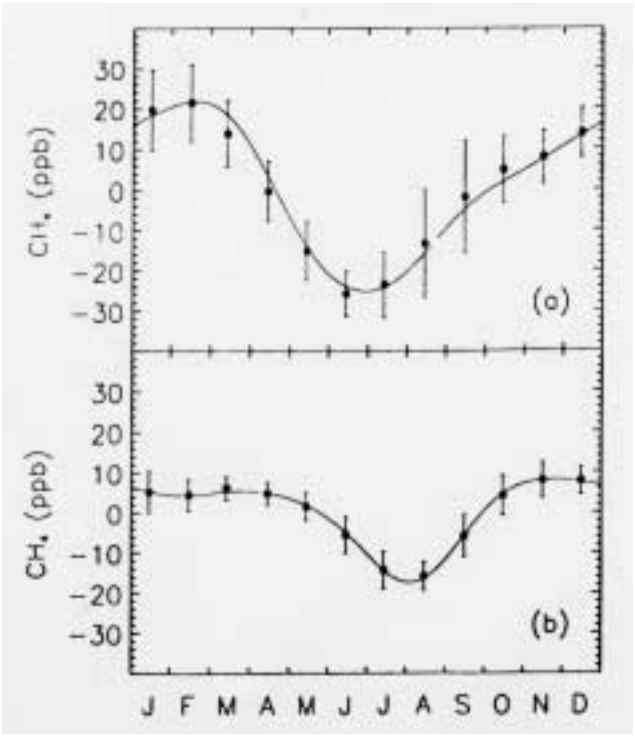

Fig. 2.10. Average seasonal cycles for BRW (*a*) and MLO (*b*) determined from the fundamental and harmonic frequencies in eq. 1. Detrended monthly means are also shown (±1s); these were determined from the smooth curve fits to complete data records for each site.